

1 **Quantitative monitoring of neuronal regeneration by functional assay and**
2 **wireless neural recording**

3 **Min-Zong Liang^{1#}, Jenq-Wei Yang^{2#}, Hsin Chen³, Mei-Yuan Cheng⁴, Linyi Chen^{1,5*}**

4 ¹ Institute of Molecular Medicine, National Tsing Hua University, Hsinchu, 300044, Taiwan

5 ² BioPro Scientific Co. Ltd., Hsinchu, 300044, Taiwan

6 ³ Department of Electrical Engineering, National Tsing Hua University, Hsinchu, 300044, Taiwan

7 ⁴ Section of Epilepsy, Department of Neurology, Chang Gung Memorial Hospital at Linkou Medical
8 Center and Chang Gung University College of Medicine, 5 Fu-Shin Street, Kwei-Shan, Taoyuan,
9 333, Taiwan

10 ⁵Department of Medical Science, National Tsing Hua University, Hsinchu, 300044, Taiwan *

11 **# Equal contribution**

12

13

14

15

16

17 *** Correspondence:**

18 Linyi Chen, PhD. Department of Medical Science, National Tsing Hua University, Hsinchu, 300044,
19 Taiwan. lchen@life.nthu.edu.tw

20 **Keywords: local field potential, brain injury, neuronal regeneration, somatosensory evoked**
21 **response, motor function.**

22

23 Abstract

24 Brain injury is heterozygous in nature and no single scheme is ideal for diagnosis and prognosis.
25 Assessing proteins in cerebrospinal fluid is limited or not applicable after surgery whereas plasma
26 biomarkers can only report occurrence of injury. The lack of regeneration markers renders the difficulty
27 during drug discovery. This study aims to establish a potential reporter that correlates the regeneration
28 progress of injured brain neurons. According to our recent publication, treatment of mitochondrial
29 uncoupler carbonyl cyanide 4-(trifluoromethoxy) phenylhydrazone (FCCP) could rescue motor
30 function deficit of mice after traumatic brain injury. We thus measured the local field potential (LFP)
31 at sites proximal to the injury region. The recorded neuronal activity reported stimulation of right
32 forelimb of mice. Our experimental results indicate that the recovery of evoked LFP correlates with
33 FCCP treatment and could potentially be used as a regeneration biomarker. These promising findings
34 suggest future application of a wireless, non-invasive recording system as a potential companion
35 diagnosis device during drug development.

36

37 Neurological dysfunctions can be caused by trauma, stroke, autoimmune disease, aging, tumor,
38 surgery, and infection. A complex set of clinical symptoms, including motor function deficit,
39 coordination, speech, cognition, learning and memory, are associated with one or more insults. Among
40 these, motor function deficit caused by traumatic brain injury (TBI) could significantly affect life
41 quality, production loss and social impairment. Nonetheless, there is currently no medicine to promote
42 neuronal regeneration after brain injury. One obstacle during drug development is the lack of
43 regeneration biomarkers, despite several brain injury markers, S100 calcium-binding protein B and
44 glial fibrillary acidic protein, have been proposed. Several imaging modalities are used to obtain the
45 necessary information for patient care and prognosis. X-ray computed tomography is used as an
46 imaging modality for assessing acute phase of TBI whereas magnetic resonance imaging is utilized in
47 subacute and chronic cases when post-concussive symptoms are persistent. However, not all imaging
48 modalities employed in TBI diagnosis reveal functional modifications. In addition, these two
49 measurements cost a lot and are not accessible at local clinic. Behavior outcome and cognitive
50 improvement have been used as measurements for drug efficacy. However, these parameters could
51 largely depend on rehabilitation over time instead of drug administration. In addition, treating TBI
52 patients early is expected to provide better outcome and reduce the development of neurodegenerative
53 diseases later in their life. Thus, establishing a system to report drug effects during the acute phase of
54 TBI is essential to facilitate drug development for treating brain injury. In this study, we used traumatic

55 brain injury mice as a biological model, aiming to correlate neural activity and behavior improvement
56 during neuronal regeneration. The local field potential (LFP) evoked by tactile stimulation is recorded
57 before and after TBI. The feasibility of using the evoked LFP to reflect the functional outcome
58 quantitatively and robustly is investigated. We shall further advance this technology toward wireless,
59 non-invasive recording system for monitoring neuronal regeneration.

60 The mitochondrial oxidative phosphorylation system transfers protons from mitochondrial matrix
61 to intermembrane space to form a proton gradient, which drives ATP synthesis (Hatefi, 1985).
62 Mitochondrial uncoupler carbonyl cyanide 4-(trifluoromethoxy) phenylhydrazone (FCCP) induces a
63 proton leak across the inner mitochondrial membrane to depolarized mitochondria. Nonetheless, it was
64 reported that optimal dosage of FCCP reduced mitochondrial dysfunction and improves cognitive
65 outcome of rat after TBI (Benz & McLaughlin, 1983; Pandya et al., 2009) . To understand the
66 mechanism and test the effect of FCCP on motor function, we have examined the effect of FCCP on
67 the cleavage of a mitochondrial protein phosphoglycerate mutase 5 and the correlation to neurite re-
68 growth of injured brain neurons. As reported recently that one dose intranasal administration of 0.1
69 mg/kg FCCP promoted mitochondrial biogenesis and neurite re-growth of injured cortical neurons
70 (Liang et al., 2023). For TBI mice, we have established controlled cortical impact (CCI) protocol on
71 left brain using C57BL/6 mice and gridwalk test was performed as a behavior assessment to determine
72 whether TBI led to foot-fault. FCCP was intranasally administered 6 hrs after CCI, numbers of foot-
73 faults of right forelimb were calculated (Fig. 1A-C). The number of foot-faults of right forelimb of CCI
74 mice treated with 0.1 mg/kg FCCP or DMSO (vehicle) were increased on 1 day post injury (dpi),
75 compared to sham mice (Fig. 1D, E), indicating that motor function of right forelimb was impaired
76 after CCI. We observed a reduction in the average number of foot-faults of right forelimb of CCI mice
77 treated with 0.1 mg/kg FCCP on 3 dpi, which became significantly decreased by 74% on 6 dpi
78 compared to mice treated with DMSO (Fig. 1F, G). These results indicate that 0.1 mg/kg FCCP
79 improves functional recovery of right forelimb foot-faults after brain injury.

80 To examine whether neuronal activity would correlate with functional recovery, we used a 4-
81 shank 32-channel multi-electrode array to measure somatosensory evoked response induced by
82 contralateral forepaw tactile stimulation. To this end, 4-shank/32-channel probes were into the forepaw
83 somatosensory area in control mice (Fig. 1H-J). The location of these probes is proximal to the future
84 injury region, which is known respond to forepaw tactile stimulation (Fig. 1K) (Auffret et al., 2018).
85 As shown in Fig. 1L, we have demonstrated successful recording of evoked LFP following

86 contralateral forepaw tactile stimulation. When comparing the LFP of different treatment groups, Sham,
87 TBI only, TBI+Vehicle, and TBI+FCCP, we selected the largest evoked LFP (in the depth between
88 300 to 400 μ m corresponding to Layer IV) for subsequent analysis (Fig. 1M). The average amplitude
89 of sensory evoked response was significantly smaller in TBI and TBI+Vehicle groups compared to that
90 in the Sham group, whereas the evoked response in TBI+FCCP group was closer to that in Sham
91 control on 3dpi (Fig. 1N). The spontaneous LFP showed the same trend as the evoked LFP (Fig. 1O-
92 P). Further analysis of frequency bands ranging from delta to gamma activity, they were reduced in
93 TBI and TBI+Vehicle groups compared to the Sham group in all frequency. Notably, FCCP treatment
94 showed a trend of recovery in the low frequency bands, delta and theta (Fig. 1Q). Higher frequency
95 bands were low in all groups due to mice in anesthesia. LFP recordings (<300 Hz) majorly represent
96 net summation of a neuronal ensemble activity surrounding the recording site related to the
97 synchronized synaptic activity, subthreshold membrane potential and spike afterpotential (Buzsáki et
98 al., 2012). The different frequency bands of LFP (known e.g., as delta, theta, alpha, beta and gamma)
99 carry the information about the brain states and related to the different behavior state. The delta
100 oscillation is associated with the deep stage 3 of NREM sleep and occurs dominantly during
101 unconscious state (Amzica & Steriade, 1998). For the animal under isoflurane anesthesia the power of
102 low frequency oscillation increased, especially delta oscillation (Aksenov et al., 2019; Baek et al.,
103 2022). Our data major represents the conditions when the animal is in sleep or unconscious stages.

104 This study used a wireless neuromodulator to record the evoked LFP, so as to monitor neuronal
105 damage and regeneration after brain injury. During neuronal regeneration, the evoked LFP correlated
106 with FCCP-promoted function recovery reliably. To reduce noise interferences, the recordings were
107 performed in anesthetized mice in this study. Following this promising study, neural activities of a
108 freely-moving TBI mice will be further recorded wirelessly with a non-invasive electrode (e.g. a
109 flexible ECoG surface electrode array) for long-term monitoring. Such experiments would help to
110 identify more natural, characteristic activities that indicate the rehabilitation of movement function
111 reliably. For neuronal damage in other brain regions, the LFP could be evoked instead by electrically
112 stimulating the upstream neurons of the injured region, and the electrical stimulation can be generated
113 by the same neuromodulator in our study. All these studies would underpin wider applications of
114 wireless, non-invasive neural recording and its potential utility in human study.

115

116

117 References

118 Aksenov, D. P., Miller, M. J., Dixon, C. J., & Wyrwicz, A. M. (2019). The effect of sevoflurane and
119 isoflurane anesthesia on single unit and local field potentials. *Experimental Brain Research*, 237(6),
120 1521–1529. <https://doi.org/10.1007/s00221-019-05528-9>

121 Amzica, F., & Steriade, M. (1998). Electrophysiological correlates of sleep delta waves.
122 *Electroencephalography and Clinical Neurophysiology*, 107(2), 69–83.
123 [https://doi.org/10.1016/S0013-4694\(98\)00051-0](https://doi.org/10.1016/S0013-4694(98)00051-0)

124 An, S., Kilb, W., & Luhmann, H. J. (2014). Sensory-Evoked and Spontaneous Gamma and Spindle
125 Bursts in Neonatal Rat Motor Cortex. *Journal of Neuroscience*, 34(33), 10870–10883.
126 <https://doi.org/10.1523/JNEUROSCI.4539-13.2014>

127 Auffret, M., Ravano, V. L., Rossi, G. M. C., Hankov, N., Petersen, M. F. A., & Petersen, C. C. H.
128 (2018). Optogenetic stimulation of cortex to map evoked whisker movements in awake head-
129 restrained mice. *Neuroscience*, 368, 199–213. <https://doi.org/10.1016/j.neuroscience.2017.04.004>

130 Baek, K., Park, C. R., Jang, S., Shim, W. H., & Kim, Y. R. (2022). Anesthetic modulations dissociate
131 neuroelectric characteristics between sensory-evoked and spontaneous activities across bilateral rat
132 somatosensory cortical laminae. *Scientific Reports*, 12(1), 11661. <https://doi.org/10.1038/s41598-022-13759-0>

134 Benz, R., & McLaughlin, S. (1983). The molecular mechanism of action of the proton ionophore
135 FCCP (carbonylcyanide p-trifluoromethoxyphenylhydrazone). *Biophysical Journal*, 41(3), 381–398.
136 [https://doi.org/10.1016/S0006-3495\(83\)84449-X](https://doi.org/10.1016/S0006-3495(83)84449-X)

137 Buzsáki, G., Anastassiou, C. A., & Koch, C. (2012). The origin of extracellular fields and currents —
138 EEG, ECoG, LFP and spikes. *Nature Reviews Neuroscience*, 13(6), 407–420.
139 <https://doi.org/10.1038/nrn3241>

140 Hanson, L. R., Fine, J. M., Svitak, A. L., & Faltesek, K. A. (2013). Intranasal Administration of CNS
141 Therapeutics to Awake Mice. *Journal of Visualized Experiments*, 74. <https://doi.org/10.3791/4440>

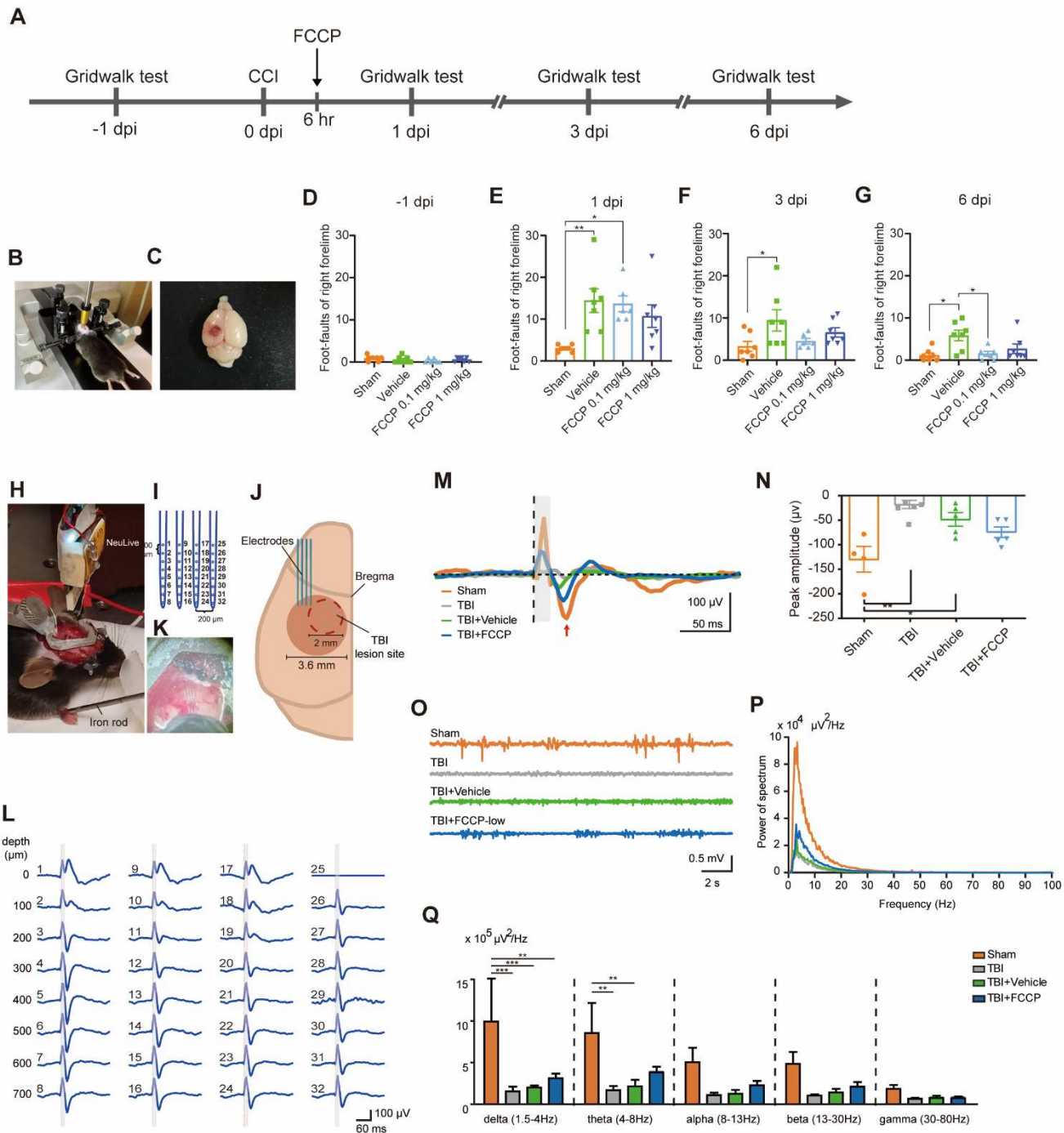
142 Hatefi, Y. (1985). THE MITOCHONDRIAL ELECTRON TRANSPORT AND OXIDATIVE
143 PHOSPHORYLATION SYSTEM. *Annual Review of Biochemistry*, 54(1), 1015–1069.
144 <https://doi.org/10.1146/annurev.bi.54.070185.005055>

145 Liang, M.-Z., Lu, T.-H., & Chen, L. (2023). Timely expression of PGAM5 and its cleavage control
146 mitochondrial homeostasis during neurite re-growth after traumatic brain injury. *Cell & Bioscience*
147 (2023) 13:96. <https://doi.org/10.1186/s13578-023-01052-0>

148 Onyszchuk, G., Al-Hafez, B., He, Y.-Y., Bilgen, M., Berman, N. E. J., & Brooks, W. M. (2007). A
149 mouse model of sensorimotor controlled cortical impact: Characterization using longitudinal
150 magnetic resonance imaging, behavioral assessments and histology. *Journal of Neuroscience*
151 *Methods*, 160(2), 187–196. <https://doi.org/10.1016/j.jneumeth.2006.09.007>

152 Pandya, J. D., Pauly, J. R., & Sullivan, P. G. (2009). The optimal dosage and window of opportunity
153 to maintain mitochondrial homeostasis following traumatic brain injury using the uncoupler FCCP.
154 *Experimental Neurology*, 218(2), 381–389. <https://doi.org/10.1016/j.expneurol.2009.05.023>

155 **Figure and legend**



156

157 **Fig. 1. Design of multi-electrode arrays for measuring LFP and reporting brain injury**

158 (A) Experimental diagram of the gridwalk test. FCCP or vehicle (DMSO) was nasally administrated
159 6 hrs after CCI. Gridwalk test was performed on -1, 1, 3 and 6 dpi to examine foot fault of CCI mice.
160 (B) Mice were impacted with CCI impactor. (C) Dissected brain of CCI mice. Scale bar, 5 mm. (D-
161 G) The number of foot-faults of right forelimb of CCI mice in 5 min. Data are presented as mean \pm
162 SEM (n = 6-7 mice/group). * p < 0.05, ** p < 0.01, one-way ANOVA with Tukey's multiple

163 comparisons. (H) A photo shows the experimental setup including a C57BL/6 mouse under light
164 isoflurane anesthesia (1.2~1.5%), a NeuLive recording head stage, a silicon based multi-electrode
165 array for LFP recording, and an iron rod for tactile stimulation. (I) A schematic illustration of the 4-
166 shank 32-channel multi-electrode array used in this study. (J) A top view photo shows the insertion
167 site of the multi-electrode array. (K) A schematic illustration of the insertion site of the multi-
168 electrode array (0.5 mm posterior and 2 to 3 mm lateral from bregma). (L) An example of the average
169 evoked LFP by tactile stimulation on the contralateral forelimb. The gray window indicates the period
170 of stimulation artifact. (M) The grand averages of evoked LFP responses following contralateral
171 forelimb tactile stimulation in different experimental conditions are shown. The onset time of
172 stimulation is indicated by a black vertical dashed line, and the gray window indicates the period of
173 stimulation artifact. The evoked LFP response is marked by a red arrow. (N) The negative peak
174 amplitude of evoked response is shown for different experimental groups. Data are presented as mean
175 \pm SEM (n = 4-5 mice/group). * p < 0.05, ** p < 0.01, one-way ANOVA with Tukey's multiple
176 comparisons. (O) An example of 20 sec spontaneous activity for different experimental groups. (P)
177 The averaged FFT spectra of 300 sec spontaneous activity in different experimental groups. (Q) The
178 summation of averaged FFT power in different frequency bands. Data are presented as mean \pm SEM
179 (n = 4-5 mice/group). * p < 0.05, ** p < 0.01, *** p < 0.001, two-way ANOVA with Tukey's multiple
180 comparisons.